# Background evolution and growth of structures in interacting dark energy scenarios through dynamical system analysis

Wompherdeiki Khyllep,[1,2,*] Jibitesh Dutta,[3,4,†] Spyros Basilakos,[5,6,‡] and Emmanuel N. Saridakis[5,7,8,§]

[1]Department of Mathematics, North-Eastern Hill University, Shillong, Meghalaya 793022, India
[2]Department of Mathematics, St. Anthony's College, Shillong, Meghalaya 793001, India
[3]Mathematics Division, Department of Basic Sciences and Social Sciences, North-Eastern Hill University, Shillong, Meghalaya 793022, India
[4]Inter University Centre for Astronomy and Astrophysics, Pune 411007, India
[5]National Observatory of Athens, Lofos Nymfon, 11852 Athens, Greece
[6]Academy of Athens, Research Center for Astronomy and Applied Mathematics, Soranou Efesiou 4, 11527, Athens, Greece
[7]CAS Key Laboratory for Researches in Galaxies and Cosmology, Department of Astronomy, University of Science and Technology of China, Hefei, Anhui 230026, People's Republic of China
[8]School of Astronomy, School of Physical Sciences, University of Science and Technology of China, Hefei 230026, People's Republic of China

(Received 10 November 2021; accepted 12 January 2022; published 8 February 2022)

We apply the formalism of dynamical system analysis to investigate the evolution of interacting dark energy scenarios at the background and perturbation levels in a unified way. Since the resulting dynamical system contains the extra perturbation variable related to the matter overdensity, the critical points of the background analysis split, corresponding to different behavior of matter perturbations and hence to stability properties. From the combined analysis, we find critical points that describe the nonaccelerating matter-dominated epoch with the correct growth of matter structure, and the fact that they are saddle provides the natural exit from this phase. Furthermore, we find stable attractors at late times corresponding to a dark energy–dominated accelerated solution with constant matter perturbations, as required by observations. Thus, interacting cosmology can describe the matter and dark energy epochs correctly, both at the background and perturbation levels, which reveals the capabilities of the interaction.

DOI: 10.1103/PhysRevD.105.043511

## I. INTRODUCTION

According to cumulative observations of different origins, the Universe is currently at a phase of accelerating expansion. Although the cosmological constant might be the simplest explanation, the corresponding problem and the possibility of a dynamical nature led to two main directions of modification. The first is to construct extended theories of gravity, which recover general relativity at low energies but which in general lead to richer cosmological evolution [1–3]. The second avenue is to introduce a new sector, collectively known as dark energy (DE) [4,5], with suitable properties that can trigger acceleration. The dynamical form of DE is usually based on scalar fields, with the simplest choice being the quintessence one. Scalar-field models usually appear in the low-energy limit of various high-energy theories, such as the string theory [6]. However, the inability to explain various observational issues has led to a plethora of scalar field constructions.

Usually, the DE component is assumed to evolve independently, coupled only to gravity and without interactions with the matter components. Nevertheless, in principle, one cannot neglect possible interactions between the DE and the dark matter (DM) component. Interacting DE-DM scenarios are capable of alleviating the cosmic coincidence problem, leading to late-time accelerated scaling attractors [7]. Additionally, more recently, it was shown that interacting models offer possible solutions to the $H_0$ and $\sigma_8$ tensions, and moreover they can alleviate the tension between cosmic microwave background and cosmic shear measurements [8–14]. As a result, there have appeared many interacting models which exhibit interesting cosmological phenomenology [15–43] (for reviews, see Refs. [44,45]) and have been confronted with detailed observational data, such as the Supernovae Type Ia, baryon acoustic oscillations, cosmic microwave background, dark energy survey, galaxy clusters, Hubble function measurements, etc., [46–55].

*sjwomkhyllep@gmail.com
†Corresponding author.
jibitesh@nehu.ac.in
‡svasil@academyofathens.gr
§msaridak@noa.gr

 

To examine the viability of a cosmological model, one has first to investigate its evolution at the background level. The next necessary step is the detailed analysis of the cosmological perturbations since these provide information on the stability of the model; they allow for a direct confrontation with growth data, and moreover, they offer a way to distinguish between different scenarios that may lead to the same background evolution [56–59]. Concerning interacting scenarios, the effect of DE-DM interaction on the growth of structures has been analyzed numerically in Ref. [60], and it was found that it affects the matter clustering [61,62]. Hence, one may observe the imprint of the interaction on structure formation, compared to the noninteracting scenario.

In general, cosmological models are determined by complicated equations, and the order of complexity increases as we shift from the background to the perturbation level. Therefore, it is required to use suitable mathematical techniques to extract analytical information and be independent of the initial conditions and the specific Universe evolution. One such powerful mathematical tool is the theory of dynamical systems analysis. In particular, the phase-space analysis allows us to bypass the complexity of the equations and extract information on the global behavior of the system by examining the corresponding critical points since the asymptotic behavior of the model is determined by its form and nature.

The dynamical system approach has been applied in the cosmological context at the background level in numerous works [63–79], including interacting cosmology [80–82]. However, at the perturbation level, it has been applied only partially in very few works [83–89]. Only recently, a dynamical system analysis of the background as well as the perturbed system was performed systematically for the Lambda Cold Dark Matter (ΛCDM) paradigm and quintessence scenario with exponential potential [90–92].

Because of the significant effects of DE-DM interaction on both the background evolution and the growth of structure, it is interesting and necessary to perform detailed dynamical system analysis on interacting cosmology at both the background and perturbation levels. In this way, we can determine the growing mode solution/trajectory determining the structure formation independent of the specific initial conditions. Additionally, we can study how the matter perturbations affect the nature of the background solutions and how perturbations evolve during the cosmological epochs described by each critical point. Finally, we can examine the sensitivity of the structure's growth rate on the strength of the interaction term.

With this motivation, in the present work, we will perform a complete dynamical system analysis of various interacting scalar field models, by combining the background and perturbation field equations. The manuscript is structured as follows. In Sec. II, we present the field equations of a general interacting scalar-field scenario, providing the equations of the background evolution as well as the ones determining the linear matter perturbations. Then, in Sec. III, we perform a detailed phase-space analysis of the full system for two interacting models. Finally, in Sec. IV, we summarize the obtained results.

## II. INTERACTING DARK ENERGY

In this section, we briefly review cosmology with dark energy–dark matter interaction, using a scalar field to describe the former. The total action of a minimally coupled scalar field in the framework of general relativity is

$$S = \int d^4x\sqrt{-g}\left[\frac{R}{2\kappa^2} + \mathcal{L}_\phi + \mathcal{L}_m\right], \tag{1}$$

where $\kappa^2$ is the gravitational constant; $g$ is the determinant of the metric $g_{\mu\nu}$; $R$ is the Ricci scalar; $\mathcal{L}_m$ and $\mathcal{L}_\phi$ are, respectively, the matter and scalar-field Lagrangian. In particular, $\mathcal{L}_\phi$ is given by

$$\mathcal{L}_\phi = -\frac{1}{2}g^{\mu\nu}\partial_\mu\phi\partial_\nu\phi - V(\phi), \qquad (\mu,\nu = 0,1,2,3), \tag{2}$$

where $V(\phi)$ is the potential for the scalar field $\phi$ and $\mathcal{L}_m$ is considered to correspond to a perfect fluid.

Variation of the action with respect to the metric leads to the field equations

$$R_{\mu\nu} - \frac{1}{2}g_{\mu\nu}R = \kappa^2(T^{(\phi)}_{\mu\nu} + T^{(m)}_{\mu\nu}), \tag{3}$$

where the scalar-field energy-momentum tensor $T^{(\phi)}_{\mu\nu}$ is given by

$$T^{(\phi)}_{\mu\nu} = \partial_\mu\phi\partial_\nu\phi - g_{\mu\nu}\left[-\frac{1}{2}g^{\alpha\beta}\partial_\alpha\phi\partial_\beta\phi + V(\phi)\right], \tag{4}$$

and the matter energy-momentum tensor $T^{(m)}_{\mu\nu}$ is given by

$$T^{(m)}_{\mu\nu} = p_m g_{\mu\nu} + (\rho_m + p_m)u_\mu u_\nu, \tag{5}$$

with $\rho_m$ and $p_m$ the energy density and pressure of the DM component, respectively.

To quantitatively describe the interaction between the DM and DE component, the total conservation equation is split as

$$\nabla_\nu T^{\mu\nu}_m = Q^\mu_m, \qquad \nabla_\nu T^{\mu\nu}_\phi = Q^\mu_\phi, \tag{6}$$

where $Q^0_\phi = -Q^0_m \equiv Q$ is the phenomenological descriptor of the interaction, denoting the rate of energy transfer between the interacting components.

### A. Cosmological equations: Background level

To proceed to cosmological applications, we consider a homogeneous and isotropic spatially flat Friedmann-Lemaître-Robertson-Walker metric of the form

$$ds^2 = -dt^2 + a^2(t)(dx^2 + dy^2 + dz^2), \tag{7}$$

in Cartesian coordinates. Under the above metric, the Einstein field equations (3) provide the two Friedmann equations,

$$3H^2 = \kappa^2(\rho_m + \rho_\phi), \tag{8}$$

$$2\dot{H} + 3H^2 = -\kappa^2(p_m + p_\phi), \tag{9}$$

where $\rho_\phi = \frac{1}{2}\dot{\phi}^2 + V$ and $p_\phi = \frac{1}{2}\dot{\phi}^2 - V$ are the scalar-field energy density and pressure, respectively, with the upper dot denoting derivative with respect to $t$. Additionally, under the metric (7), the conservation equations (6) become

$$\dot{\rho}_\phi + 3H(\rho_\phi + p_\phi) = Q, \tag{10}$$

$$\dot{\rho}_m + 3H(1+w)\rho_m = -Q, \tag{11}$$

where $w \equiv p_m/\rho_m$ is the equation of state of DM. Hence, one can see that $Q > 0$ corresponds to energy flow from dark matter to dark energy, while $Q < 0$ corresponds to energy transfer in the opposite direction.

We can introduce the density parameters for the two sectors as

$$\Omega_\phi \equiv \frac{\kappa^2\rho_\phi}{3H^2} = \frac{\kappa^2\dot{\phi}^2}{6H^2} + \frac{\kappa^2 V}{3H^2}, \tag{12}$$

$$\Omega_m \equiv \frac{\kappa^2\rho_m}{3H^2}, \tag{13}$$

and thus the Friedmann equation (8) becomes

$$\Omega_m + \Omega_\phi = 1. \tag{14}$$

Finally, it proves convenient to define the total, effective, equation-of-state parameter $w_{\rm eff}$ as

$$w_{\rm eff} = \frac{p_\phi + p_m}{\rho_\phi + \rho_m} = \frac{\frac{1}{2}\dot{\phi}^2 - V + w\rho_m}{\frac{1}{2}\dot{\phi}^2 + V + \rho_m}, \tag{15}$$

which is related to the deceleration parameter $q$ as $w_{\rm eff} = \frac{2q-1}{3}$. As usual, to have acceleration, one requires the condition $w_{\rm eff} < -\frac{1}{3}$.

### B. Cosmological equations: Linear perturbation level

We can now examine the behavior of the cosmological system at the linear perturbation level. We consider scalar perturbations in the Newtonian gauge, namely,

$$ds^2 = -(1+2\Phi)dt^2 + a^2(1-2\Phi)(dx^2 + dy^2 + dz^2), \tag{16}$$

and since we are interested in the late-time behavior, we have ignored the anisotropic stress. We decompose the matter energy density $\bar{\rho}_m$, the matter 4-velocity $\bar{u}_\mu$, the scalar field $\bar{\phi}$, and the energy transfer rate $\bar{Q}_A$ into background values and perturbations as

$$\begin{aligned} \bar{\rho}_m &= \rho_m + \delta\rho_m, \\ \bar{u}_\mu &= u_\mu + \delta u_\mu, \\ \bar{\phi} &= \phi + \delta\phi, \\ \bar{Q} &= Q + \delta Q. \end{aligned} \tag{17}$$

In this work, we focus on the observationally interesting matter perturbations, and thus we will not consider the DE ones, since the latter can be assumed to have a high sound speed and thus does not cluster. Therefore, the evolution equations for the DM energy density perturbation $\delta = \delta\rho_m/\rho_m$ and the divergence of velocity perturbations $\theta$ in the Fourier space are [93–96]

$$\dot{\delta} + \left[3H(c_s^2 - w) - \frac{Q}{\rho}\right]\delta + (1+w)(\theta - 3\dot{\Phi}) = -\frac{\delta Q}{\rho}, \tag{18}$$

$$\dot{\theta} + \left[H(1-3w) - \frac{Q}{\rho} + \frac{\dot{w}}{1+w}\right]\theta - k^2\Phi - \frac{c_s^2}{1+w}k^2\delta = 0, \tag{19}$$

where $c_s^2$ is the sound speed of the fluid, $\theta = a^{-1}ik^j\delta u_j$ is the divergence of the velocity perturbation, and $k^j$ the wave vector component. Finally, to analyze the behavior of DM perturbations, one has to combine Eqs. (18) and (19), with the help of the Poisson equation [90]. Since structures grow in scales much smaller than the Hubble radius $H^{-1}$ (i.e., $k \gg aH$), the Poisson equation becomes

$$k^2\Phi = -\frac{3}{2}H^2\Omega_m\delta. \tag{20}$$

## III. DYNAMICAL SYSTEM ANALYSIS

In this section, we shall perform a full dynamical system analysis in order to investigate interacting cosmology. Without loss of generality, we will focus on two well-studied simple interacting models, namely, $Q = \alpha H\rho_m$ and $Q = \Gamma\rho_m$. Moreover, concerning the matter sector, as usual, we assume it to be dust, i.e., with $w = 0$, while for the scalar field potential, we focus on the usual exponential potential $V(\phi) = V_0 e^{-\lambda\phi}$, with $V_0 > 0$ and

where $\lambda$ is a dimensionless parameter. The dynamical system analysis at the background level is performed in Refs. [80,82]; however, in the present work, we extend the analysis by taking into account the effect of perturbations.

### A. Interacting model I: $Q = \alpha H \rho_m$

The simple interacting model with $Q = \alpha H \rho_m$, where $\alpha$ is the dimensionless model parameter, has been mathematically designed to provide accelerated scaling attractors, which can alleviate the coincidence problem [80,82]. The sign of $\alpha$ determines the energy transfer direction, i.e., $\alpha > 0$ corresponds to energy flow from matter to DE, and vice versa.

Inserting $Q = \alpha H \rho_m$ into (18) leads to $\delta Q = \alpha \rho_m \delta H + \alpha H \delta \rho_m$, and $\delta H$ is then expressed in terms of $\Phi$. Nevertheless, as it was found in Refs. [19,22,94,97–99], the consideration of $\delta H$ terms does not have a significant quantitative difference in matter overdensity evolution (which is the observable that we are interested in the present work), in comparison to the case where $\delta H$ terms are neglected. Hence, in the following, we do not consider these terms. Therefore, the evolution of DM perturbations obtained from Eqs. (18), (19), and (20) can be approximated by

$$\ddot{\delta} + (2 + 3\alpha) H \dot{\delta} - \frac{3}{2} \Omega_m H^2 \delta = 0. \tag{21}$$

We now proceed to the investigation of perturbations by considering the above perturbed equation along with the background equations (8)–(11). Since we are interested in the qualitative behavior of $\delta$, we recast the equations into a first-order autonomous system by considering the following auxiliary variables [90]:

$$x = \frac{\kappa \dot{\phi}}{\sqrt{6} H}, \qquad y = \frac{\kappa \sqrt{V}}{\sqrt{3} H}, \qquad U = \frac{d(\ln \delta)}{d(\ln a)}. \tag{22}$$

Note that the variables $x$, $y$ correspond to the background behavior of the Universe, while variable $U$ is the usual growth rate which quantifies the perturbation growth. A positive $U$ indicates that inhomogeneities grow, while negative $U$ indicates inhomogeneities decay whenever perturbation $\delta$ is positive. In terms of the above variables, the background cosmological quantities $\Omega_\phi$, $\Omega_m$, and $w_{\rm eff}$ can be written as

$$\begin{aligned} \Omega_\phi &= x^2 + y^2, \\ \Omega_m &= 1 - (x^2 + y^2), \\ w_{\rm eff} &= x^2 - y^2. \end{aligned} \tag{23}$$

Hence, under the variables (22), the cosmological equations of the present scenario can be expressed in the form of the dynamical system

$$x' = -3x + \frac{\sqrt{6}}{2} \lambda y^2 + \frac{3}{2} x (1 + x^2 - y^2) + \alpha \frac{(1 - x^2 - y^2)}{2x}, \tag{24}$$

$$y' = -\frac{\sqrt{6}}{2} \lambda x y + \frac{3}{2} y (1 + x^2 - y^2), \tag{25}$$

$$U' = -U(U + 2 + 3\alpha) + \frac{3}{2}(1 - x^2 - y^2) + \frac{3}{2}(1 + x^2 - y^2) U, \tag{26}$$

where primes denote derivatives with respect to $\ln a$ (note that in this notation we have simply that $U = \frac{\delta'}{\delta}$).

Since we study the expanding universe and since the system (24)–(26) is invariant under a transformation $y \to -y$, we focus only on the phase-space region $y \geq 0$. Additionally, from the physical condition $0 \leq \Omega_m \leq 1$, the background variables $x$ and $y$ are restricted within the circle $x^2 + y^2 = 1$. In summary, the background phase space $\mathbb{B}$ consists of the variables $x$, $y$, while the perturbation phase space $\mathbb{P}$ consists of $U$, and hence the phase space of the system (24)–(26) is the product space $\mathbb{B} \times \mathbb{P}$ given by

$$\begin{aligned} \mathbb{B} \times \mathbb{P} = \{ (x, y, U) \in \mathbb{R}^2 \times \mathbb{R} : & 0 \leq x^2 + y^2 \leq 1, \\ & -1 \leq x \leq 1, 0 \leq y \leq 1 \}. \end{aligned} \tag{27}$$

We mention here that the background equations (24)–(25) on the background space $\mathbb{B}$ are decoupled from the perturbation equation (26) on $\mathbb{P}$, and as usual, the projection of an orbit in the product space $\mathbb{B} \times \mathbb{P}$ on the background space reduces to the corresponding orbit on $\mathbb{B}$.

We proceed to an extraction of critical points of the system (24)–(26), by equating the right-hand side of the equations to zero. Then, to determine the stability of these points, we calculate the eigenvalues of the Jacobian matrix associated with them [63,64]. On the physical grounds, a stable background point with $U > 0$ implies that the matter perturbations grow indefinitely, indicating the instability of the system with respect to matter perturbations. On the contrary, a stable background point with $U < 0$ implies that the matter perturbations will eventually decay, indicating the asymptotical stability of the system with respect to matter perturbations. Finally, when $U = 0$ for a stable background point, it implies that the matter perturbations of the system asymptotically tend to a fixed value.

In Table I, we summarize the physical critical points of the scenario, alongside their existence and stability conditions, as well as the values for the observable quantities $\Omega_m$ and $w_{\rm eff}$, while in Table II, we give the associated eigenvalues. As expected, the inclusion of scalar perturbations leads to the split of each critical point of the background analysis into two distinct points, i.e., points that have the same background coordinates $x$ and $y$ but different perturbation coordinate $U$. Hence, the dynamical system

TABLE I. The critical points of the system (24)–(26), for the interacting model I, namely, with $Q = \alpha H \rho_m$, alongside their existence and stability conditions, and the values of the matter density parameter $\Omega_m$ and the total, effective, equation-of-state parameter $w_{\rm eff}$.

| Point | $x$ | $y$ | $U$ | Existence | Stability | $\Omega_m$ | $w_{\rm eff}$ |
|---|---|---|---|---|---|---|---|
| $A_\pm$ | $\pm 1$ | 0 | 0 | Always | Unstable node for $\alpha < 1, \pm\lambda < \sqrt{6}$<br>Stable node for $\alpha > 3, \pm\lambda > \sqrt{6}$<br>Saddle otherwise | 0 | 1 |
| $B_\pm$ | $\pm 1$ | 0 | $1-\alpha$ | Always | Unstable node for $1 < \alpha < 3$, $\pm\lambda < \sqrt{6}$<br>Saddle otherwise | 0 | 1 |
| $C$ | $\frac{\lambda}{\sqrt{6}}$ | $\sqrt{1-\frac{\lambda^2}{6}}$ | 0 | $\lambda^2 \leq 6$ | Stable node for $\alpha > \lambda^2 - 3$, $\alpha > \frac{\lambda^2}{2} - 2$<br>Saddle otherwise | 0 | $\frac{\lambda^2}{3} - 1$ |
| $D$ | $\frac{\lambda}{\sqrt{6}}$ | $\sqrt{1-\frac{\lambda^2}{6}}$ | $\frac{\lambda^2}{2} - \alpha - 2$ | $\lambda^2 \leq 6$ | Stable node for $\alpha > \lambda^2 - 3$ or $\alpha < \frac{\lambda^2}{2} - 2$<br>Saddle otherwise | 0 | $\frac{\lambda^2}{3} - 1$ |
| $E_\pm$ | $\frac{\alpha+3}{\sqrt{6}\lambda}$ | $\frac{\sqrt{(\alpha+3)^2 - 2\alpha\lambda^2}}{\sqrt{6}\lambda}$ | $-\frac{1}{4}(\alpha+1) \pm \frac{\sqrt{\lambda^2(\alpha+5)^2 - 8(\alpha+3)^2}}{4\lambda}$ | $2\alpha \leq \frac{(\alpha+3)^2}{\lambda^2} \leq \frac{(\alpha+5)^2}{8}$ | See Fig. 1 | $\frac{(\alpha+3)(\lambda^2-\alpha-3)}{3\lambda^2}$ | $\frac{\alpha}{3}$ |
| $F_\pm$ | $\frac{\sqrt{\alpha}}{\sqrt{3}}$ | 0 | $-\frac{1}{4}(\alpha+1) \pm \frac{1}{4}\sqrt{(\alpha-3)^2 + 16}$ | $\alpha \geq 0$ | $F_+$ stable for $\lambda\sqrt{2\alpha} > \alpha + 3$<br>Saddle otherwise<br>$F_-$ saddle always | $1 - \frac{\alpha}{3}$ | $\frac{\alpha}{3}$ |
| $G_\pm$ | $-\frac{\sqrt{\alpha}}{\sqrt{3}}$ | 0 | $-\frac{1}{4}(\alpha+1) \pm \frac{1}{4}\sqrt{(\alpha-3)^2 + 16}$ | $\alpha \geq 0$ | $G_+$ stable for $\lambda\sqrt{2\alpha} < -\alpha + 3$<br>Saddle otherwise<br>$G_-$ saddle always | $1 - \frac{\alpha}{3}$ | $\frac{\alpha}{3}$ |

analysis can offer us information on the behavior of matter perturbations at these critical points, namely, whether they are growing, decaying, or remaining constant. In particular:

(i) Points $A_\pm$ correspond to DE-dominated solutions, with a stiff total equation of state, and thus are not favored by observations, and with a constant matter perturbation $U = 0$. Point $A_+$ is unstable node when $\alpha < 1$ and $\lambda < \sqrt{6}$ and stable when $\alpha > 3$ and $\lambda > \sqrt{6}$; otherwise, it is saddle. Point $A_-$ is unstable node when $\alpha < 1$ and $\lambda > -\sqrt{6}$, stable when $\alpha > 3$ and $\lambda < -\sqrt{6}$, and saddle otherwise.

(ii) Points $B_\pm$ also correspond to stiff DE-dominated solutions, and thus are not favored by observations, with the evolution of matter perturbations depending on the coupling parameter $\alpha$. For $\alpha < 1$, we have a growing mode of evolution; $\alpha > 1$ corresponds to a decaying mode of solution; and $\alpha = 1$ corresponds to a constant matter perturbation case. Point $B_+$ is an unstable node when $1 < \alpha < 3$ and $\lambda < \sqrt{6}$; otherwise, it is saddle. Similarly, point $B_-$ is an unstable node when $1 < \alpha < 3$ and $\lambda > -\sqrt{6}$ and saddle otherwise.

(iii) Point $C$ corresponds to a DE-dominated epoch and exists only for $\lambda^2 < 6$. Its effective equation of state becomes less than $-1/3$ for $\lambda^2 < 2$, giving rise to an accelerating universe. The point is stable when $\alpha > \lambda^2 - 3$ and $\alpha > \frac{\lambda^2}{2} - 2$. Additionally, it has a constant matter perturbation, i.e., $U = 0$. Hence, this point can describe the late-time Universe.

(iv) At the background level, point $D$ coincides with $C$. It corresponds to a DE-dominated epoch which is accelerating for $\lambda^2 < 2$. However, when perturbations are considered, point $D$ presents a different behavior. In particular, it can have either growing matter perturbations ($U > 0$), decaying ($U < 0$), or constant ones ($U = 0$ which happens for $\alpha = \frac{\lambda^2}{2} - 2$), even when it corresponds to a stable late-time DE-dominated universe. This makes it the

TABLE II. The eigenvalues associated with the critical points of the system (24)–(26), for the interacting model I, namely, with $Q = \alpha H \rho_m$. We have defined $\Delta_\pm = \frac{\lambda(-2\alpha\lambda^2 + 3\alpha^2 + 6\alpha - 9) \pm \sqrt{S}}{4(\alpha+3)\lambda}$, and $S = 4\alpha^2\lambda^6 + 4\alpha^3\lambda^4 - 15\alpha^4\lambda^2 + 72\alpha^2\lambda^4 + 8\alpha^5 - 204\alpha^3\lambda^2 + 180\alpha\lambda^4 + 120\alpha^4 - 882\alpha^2\lambda^2 + 720\alpha^3 - 1404\alpha\lambda^2 + 2160\alpha^2 - 567\lambda^2 + 3240\alpha + 1944$.

| Point | $E_1$ | $E_2$ | $E_3$ |
|---|---|---|---|
| $A_\pm$ | $3 - \alpha$ | $3 \mp \frac{\sqrt{6}}{2}\lambda$ | $1 - \alpha$ |
| $B_\pm$ | $3 - \alpha$ | $3 \mp \frac{\sqrt{6}}{2}\lambda$ | $\alpha - 1$ |
| $C$ | $\frac{\lambda^2}{2} - 3$ | $\lambda^2 - \alpha - 3$ | $\frac{\lambda^2}{2} - \alpha - 2$ |
| $D$ | $\frac{\lambda^2}{2} - 3$ | $\lambda^2 - \alpha - 3$ | $-\frac{\lambda^2}{2} + \alpha + 2$ |
| $E_\pm$ | $\Delta_+$ | $\Delta_-$ | $\mp\frac{\sqrt{\lambda^2(\alpha+5)^2 - 8(\alpha+3)^2}}{2\lambda}$ |
| $F_\pm$ | $\alpha - 3$ | $\frac{1}{2}(\alpha + 3 - \lambda\sqrt{2\alpha})$ | $\mp\sqrt{(\alpha-3)^2 + 16}$ |
| $G_\pm$ | $\alpha - 3$ | $\frac{1}{2}(\alpha + 3 + \lambda\sqrt{2\alpha})$ | $\mp\sqrt{(\alpha-3)^2 + 16}$ |

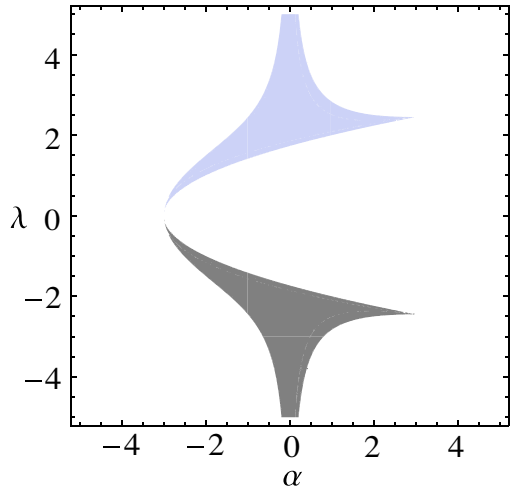


FIG. 1. Stability regions of points $E_+$ (purple) and $E_-$ (gray) in $(\alpha, \lambda)$ parameter space, for the interacting model I, namely, with $Q = \alpha H \rho_m$.

candidate for the description of the late-time Universe both at background and perturbation levels.

(v) Since the eigenvalues corresponding to points $E_\pm$ are complicated, we need to examine their behavior numerically in order to conclude on the stability of $E_\pm$. In Fig. 1, we depict the regions in the parameter space that correspond to stable behavior. Note that for $\lambda > 0$ only point $E_+$ and for $\lambda < 0$ only point $E_-$ correspond to stable solutions, and within these stable regions, both points correspond to accelerated solutions if $\alpha < -1$. Concerning the evolution of matter perturbations, in both points, $U$ can lie between 0 and 1, corresponding to growth, for particular parameter regions.

(vi) Points $F_\pm$ and $G_\pm$ are physical for $0 \leq \alpha \leq 3$, and they correspond to decelerated scaling solutions. Point $F_+$ is stable when $\lambda\sqrt{2\alpha} > \alpha + 3$; otherwise, it is saddle. Point $G_+$ is stable when $\lambda\sqrt{2\alpha} < -\alpha + 3$; otherwise, it is saddle. It is worth noting that for small $\alpha$ all four points correspond to matter-dominated solutions at the background level. Both points $F_-$ and $G_-$ are saddle within their physical regions, with decaying matter perturbations. However, points $F_+$ and $G_+$ for $\alpha < 3$ correspond to growth of matter perturbations, with $\delta \sim a$. As $\alpha$ increases, the growth rate is smaller than the usual rate during matter domination, and this reveals the effect of the coupling toward the structure formation. In summary, taking into account both the background and perturbation levels, points $F_+$ and $G_+$ are the ones that describe the structure formation.

As we observe, our analysis allows us to view different modes of matter perturbations in terms of critical points. Points that are the same at the background level analysis correspond to different behavior of matter perturbations. From the combined analysis of the background and perturbation equations, we find that points $E_-$, $F_+$, and $G_+$ are the ones that describe the nonaccelerating matter-dominated epoch with the correct growth of matter structure, and the fact that they are saddle provides the natural exit from this phase. At late times, the physically interesting points are $C$ and $D$, since they correspond to dark energy–dominated accelerated solutions with constant matter perturbations ($C$ always while $D$ for $\alpha = \frac{\lambda^2}{2} - 2$), as it is required by observations. Hence, the present scenario of

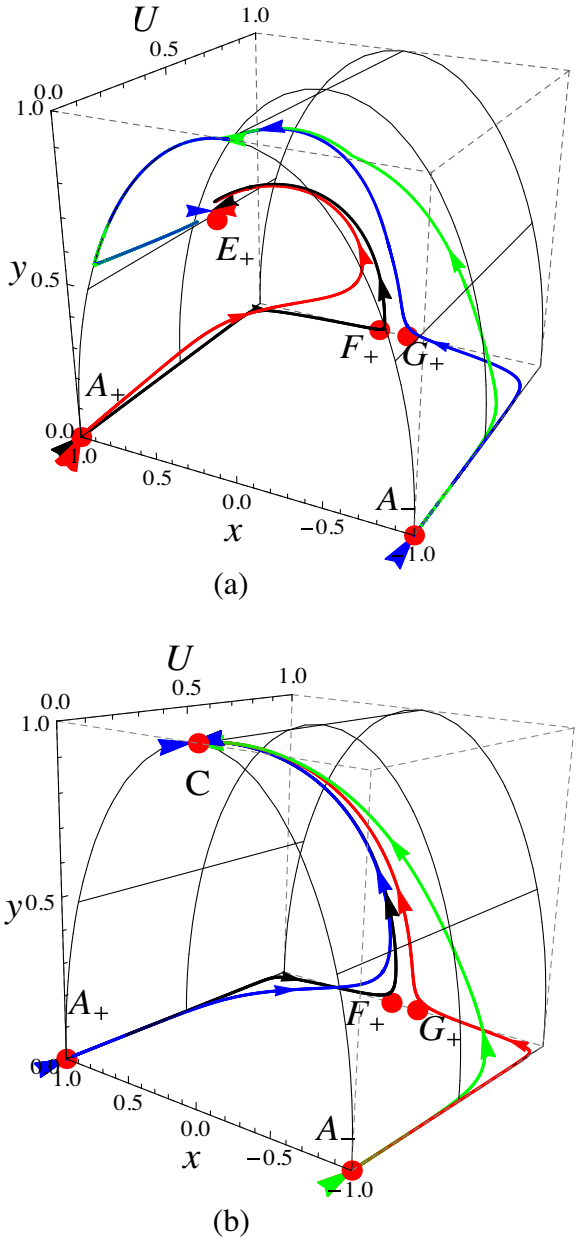


FIG. 2. The phase portrait of the system (24)–(26) of the interacting model I, namely, with $Q = \alpha H \rho_m$. Upper graph: $\alpha = 0.01$, $\lambda = 2$, and point $E_+$ is the attractor. Lower graph: $\alpha = 0.01$, $\lambda = 0.1$, and point $C$ is the attractor.

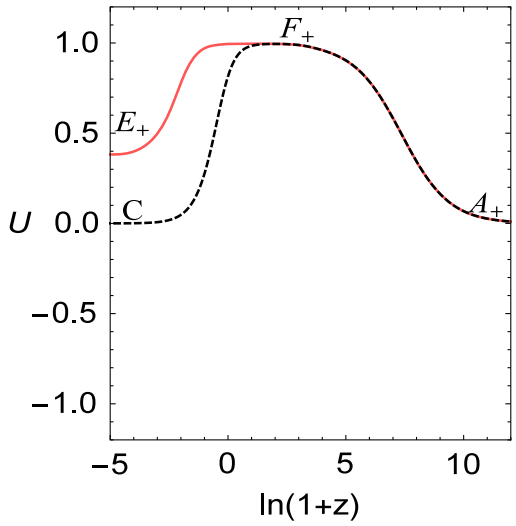


FIG. 3. The evolution of the perturbation quantity $U$ (growth rate) for the system (24)–(26) of the interacting model I, namely, with $Q = \alpha H \rho_m$, with $\alpha = 0.01$ and for $\lambda = 2$ (red solid) and $\lambda = 0.1$ (black dashed). The red-solid curve corresponds to the transition $A_+ \to F_+ \to E_+$, and the black-dashed curve corresponds to the transition $A_+ \to F_+ \to C$.

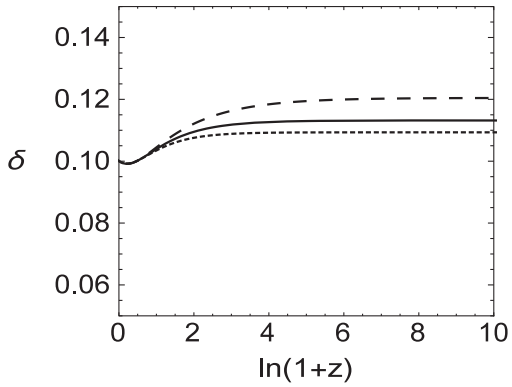


FIG. 4. The evolution of the matter overdensity $\delta$ for the interacting model I, namely, with $Q = \alpha H \rho_m$, for $\lambda = 0.2$ and with $\alpha = -0.1$ (dotted), $\alpha = 0$ (solid), and $\alpha = 0.1$ (dashed), normalized in the same final value.

interacting cosmology can describe the thermal history of the Universe correctly, both at the background and perturbation levels.

In summary, the scenario at hand can describe both an intermediate epoch with the growth of matter perturbations and a late-time accelerating epoch with constant matter perturbations, offering the correct thermal history of the Universe, at both background and perturbation levels. This is the main result of the present work, and it reveals the crucial effect of the interaction.

To be more transparent, in Fig. 2, we present the phase-space evolution of the system (24)–(26), for two cases, where we have shown only the growing mode solution of the system. Furthermore, in Fig. 3, we depict the evolution of the perturbation variable $U$, i.e., the growth rate, for two different scenarios: $A_+ \to F_+ \to E_+$ (red-solid curve) describing a transition from stiff matter to matter domination and eventually toward a decelerated scaling solution, and a sequence $A_+ \to F_+ \to C$ (black-dashed curve) describing a transition from a stiff matter to matter domination and eventually toward an accelerated dark energy–dominated solution. Since $U \geq 0$ at intermediate redshifts, we deduce that whenever $\delta > 0$, $\delta'$ is also nonnegative and thus $\delta$ is growing throughout the evolution, while at late times, according to the parameter values, the growth of perturbation stops, and the Universe enters the DE-dominated epoch. Note that the precise evolution of matter growth depends on the interaction parameter $\alpha$.

Finally, in Fig. 4, we show the evolution of the matter overdensity in the present interacting model, and we compare it with the noninteracting case. Imposing the same final conditions in the current Universe, we find that for $\alpha < 0$ at early times the matter perturbation is smaller compared to the noninteracting case. Therefore, the growth rate of structures for $\alpha < 0$ is enhanced in comparison to the noninteracting scenario, which was expected since in this case DE transforms into DM. On the other hand, the model with $\alpha > 0$ exhibits a suppressed structure growth rate.

Lastly, for completeness, we have also examined the possibility of critical points at infinity. Since, all variables apart from $U$ are bounded, we consider the transformation $U \to U_\infty$ as $U_\infty = \tan^{-1} U$ with $-\frac{\pi}{2} < U_\infty < \frac{\pi}{2}$. Nevertheless, we find that there is not any extra critical point at infinity.

### B. Interacting model II: $Q = \Gamma \rho_m$

In this subsection, we investigate an interacting model where the energy transfer rate is determined by the local transfer rate $\Gamma$, which is directly associated with the particle or field interactions. This model was used to describe the decay of DM to radiation [100,101], the decay of the curvaton field to radiation [102], and the decay of DM superheavy particles to quintessence field [103]. The fact that the interaction rate does not depend on $H$, like the model of the previous subsection, as well as similar ones, which is a global feature of the Universe, might make the present model more physical since the interaction rate is expected to be determined by local quantities. The sign of the constant $\Gamma$ determines the energy transfer direction, with the case $\Gamma > 0$ corresponding to the decay of matter to the scalar field, while the case $\Gamma < 0$ corresponds to the energy flow in the opposite direction.

Interestingly enough, due to term cancellation, the evolution of DM perturbations obtained from Eqs. (18), (19), and (20) for this model is

$$\ddot{\delta} + 2H\dot{\delta} - \frac{3}{2}\Omega_m H^2 \delta = 0, \tag{28}$$

TABLE III. The critical points of the system (29)–(32), for the interacting model II, namely, with $Q = \Gamma\rho_m$, alongside their existence and stability conditions, and the values of the matter density parameter $\Omega_m$ and the total, effective, equation-of-state parameter $w_{\rm eff}$.

| Point | $x$ | $y$ | $\zeta$ | $U$ | Existence | Stability | $\Omega_m$ | $w_{\rm eff}$ |
|---|---|---|---|---|---|---|---|---|
| $\mathcal{A}_\pm$ | $\pm1$ | 0 | 0 | 1 | Always | Saddle | 0 | 1 |
| $\mathcal{B}_\pm$ | $\pm1$ | 0 | 0 | 0 | Always | Saddle | 0 | 1 |
| $\mathcal{C}$ | $\frac{\lambda}{\sqrt{6}}$ | $\sqrt{1-\frac{\lambda^2}{6}}$ | 0 | 0 | $\lambda^2 \leq 6$ | Saddle | 0 | $\frac{\lambda^2}{3}-1$ |
| $\mathcal{D}$ | $\frac{\lambda}{\sqrt{6}}$ | $\sqrt{1-\frac{\lambda^2}{6}}$ | 0 | $\frac{\lambda^2}{2}-2$ | $\lambda^2 \leq 6$ | Saddle | 0 | $\frac{\lambda^2}{3}-1$ |
| $\mathcal{E}_\pm$ | $\frac{\sqrt{6}}{2\lambda}$ | $\frac{\sqrt{6}}{2\lambda}$ | 0 | $-\frac{1}{4}(1\pm\sqrt{25-\frac{72}{\lambda^2}})$ | $\lambda^2 \geq \frac{72}{25}$ | Saddle | $1-\frac{3}{\lambda^2}$ | 0 |
| $\mathcal{F}_\pm$ | $\pm1$ | 0 | 1 | 0 | Always | Saddle | 0 | 1 |
| $\mathcal{G}_\pm$ | $\pm1$ | 0 | 1 | 1 | Always | Stable node for $\pm\lambda > \sqrt{6}$, $\gamma > 0$<br>Saddle otherwise | 0 | 1 |
| $\mathcal{H}$ | $\frac{\lambda}{\sqrt{6}}$ | $\sqrt{1-\frac{\lambda^2}{6}}$ | 1 | 0 | $\lambda^2 \leq 6$ | Stable node for $\lambda^2 < 4$, $\gamma > 0$<br>Saddle otherwise | 0 | $\frac{\lambda^2}{3}-1$ |
| $\mathcal{I}$ | $\frac{\lambda}{\sqrt{6}}$ | $\sqrt{1-\frac{\lambda^2}{6}}$ | 1 | $\frac{\lambda^2}{2}-2$ | $\lambda^2 \leq 6$ | Stable node for $4 < \lambda^2 < 6$, $\gamma > 0$<br>Saddle otherwise | 0 | $\frac{\lambda^2}{3}-1$ |

and therefore it coincides with that of the noninteracting case. However, since the interaction does affect the background evolution, by changing the evolution of $H$ and $\Omega_m$ comparing to the noninteracting case, at the end of the day, the matter density does evolve differently in the interacting and noninteracting scenarios.

To transform the cosmological equations into an autonomous form, apart from the variables (22), we need to introduce the additional variable $\zeta = \frac{H_0}{H_0+H}$ [82], with $H_0$ the present Hubble constant. Under the variables (22) and $\zeta$, the equations of the present model can be expressed as the dynamical system

$$x' = -3x + \frac{\sqrt{6}}{2}\lambda y^2 + \frac{3}{2}x(1+x^2-y^2) - \gamma\frac{(1-x^2-y^2)\zeta}{2x(\zeta-1)}, \tag{29}$$

$$y' = -\frac{\sqrt{6}}{2}\lambda xy + \frac{3}{2}y(1+x^2-y^2), \tag{30}$$

$$\zeta' = \frac{3}{2}\zeta(1-\zeta)(1+x^2-y^2), \tag{31}$$

$$U' = -U(U+2) + \frac{3}{2}(1-x^2-y^2) + \frac{3}{2}(1+x^2-y^2)U, \tag{32}$$

where $\gamma = \frac{\Gamma}{H_0}$. For an expanding Universe ($H > 0$), the variable $\zeta$ lies between 0 and 1. Therefore, the phase space of the system (29)–(32) is the product space of the background phase space $\mathbb{B}$ consisting of the variables $x$, $y$, $\zeta$, and perturbation phase space $\mathbb{P}$ with variable $U$, given by

$$\mathbb{B}\times\mathbb{P} = \{(x,y,\zeta,U)\in\mathbb{R}^3\times\mathbb{R}: 0 \leq x^2+y^2 \leq 1, -1 \leq x \leq 1, 0 \leq y \leq 1, 0 \leq \zeta \leq 1\}. \tag{33}$$

We extract the critical points of the system (29)–(32), and we determine their features and stability by examining the sign of the corresponding eigenvalues. In Table III, we summarize the physical critical points, alongside the values for the observable quantities $\Omega_m$ and $w_{\rm eff}$, and in Table IV, we provide the associated eigenvalues. In particular:

(i) Points $\mathcal{A}_\pm$ and $\mathcal{B}_\pm$ correspond to stiff DE-dominated solutions. At the background level, these points are unstable nodes, but including the perturbation level, the points become saddle. Moreover, by considering linear perturbations, points $\mathcal{A}_\pm$ show a growth of matter perturbations of the form $\delta \sim a$ even though $\Omega_m = 0$.

TABLE IV. The eigenvalues associated with the critical points of the system (29)–(32), for the interacting model II, namely, with $Q = \Gamma\rho_m$.

| Point | $E_1$ | $E_2$ | $E_3$ | $E_4$ |
|---|---|---|---|---|
| $\mathcal{A}_\pm$ | 3 | 3 | $3\mp\frac{\sqrt{6}\lambda}{2}$ | $-1$ |
| $\mathcal{B}_\pm$ | 3 | 3 | $3\mp\frac{\sqrt{6}\lambda}{2}$ | $-1$ |
| $\mathcal{C}$ | $\frac{\lambda^2}{2}$ | $\lambda^2-3$ | $\frac{\lambda^2}{2}-3$ | $\frac{\lambda^2}{2}-2$ |
| $\mathcal{D}$ | $\frac{\lambda^2}{2}$ | $\lambda^2-3$ | $\frac{\lambda^2}{2}-3$ | $-\frac{\lambda^2}{2}+2$ |
| $\mathcal{E}_\pm$ | $\frac{3}{2}$ | $-\frac{3}{4\lambda}(\lambda+\sqrt{24-7\lambda^2})$ | $-\frac{3}{4\lambda}(\lambda-\sqrt{24-7\lambda^2})$ | $\mp\frac{\sqrt{25\lambda^2-72}}{2\lambda}$ |
| $\mathcal{F}_\pm$ | $-3$ | $3\mp\frac{\sqrt{6}\lambda}{2}$ | $-\mathrm{sgn}(\gamma)\infty$ | 1 |
| $\mathcal{G}_\pm$ | $-3$ | $3\mp\frac{\sqrt{6}\lambda}{2}$ | $-\mathrm{sgn}(\gamma)\infty$ | $-1$ |
| $\mathcal{H}$ | $-\frac{\lambda^2}{2}$ | $\frac{\lambda^2}{2}-3$ | $-\mathrm{sgn}(\gamma)\infty$ | $\frac{\lambda^2}{2}-2$ |
| $\mathcal{I}$ | $-\frac{\lambda^2}{2}$ | $\frac{\lambda^2}{2}-3$ | $-\mathrm{sgn}(\gamma)\infty$ | $-\frac{\lambda^2}{2}+2$ |

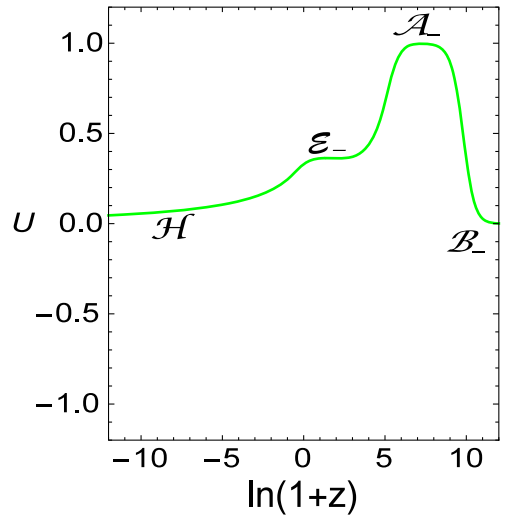


FIG. 5. The evolution of the perturbation quantity $U$ (growth rate) for the system (29)–(32) of the interacting model II, namely, with $Q = \Gamma\rho_m$, with $\lambda^2 = 3.9$, and for $\gamma = 10^{-5}$. It corresponds to the transition $\mathcal{B}_- \to \mathcal{A}_- \to \mathcal{E}_- \to \mathcal{H}$.

(ii) Points $\mathcal{C}$ and $\mathcal{D}$ correspond to DE-dominated solutions and are always saddle. Their effective equation of state becomes less than $-1/3$ for $\lambda^2 < 2$, giving rise to an accelerating universe. Nevertheless, although the two points coincide at the background level, at the level of perturbations, they differ, and in particular, point $\mathcal{C}$ has constant matter perturbations i.e., $U = 0$, while point $\mathcal{D}$ corresponds to either growth or decay of matter perturbations.

(iii) Points $\mathcal{E}_\pm$ correspond to scaling matter-dominated, nonaccelerating solutions. At the perturbation level, the growth rate of matter perturbations is smaller than the standard matter-dominated epoch. Point $\mathcal{E}_+$ corresponds to decaying matter perturbations. However, point $\mathcal{E}_-$ for $\lambda > 3$ corresponds to the growth of matter perturbations, and especially for large values of $\lambda$, it describes a matter-dominated era with matter overdensity evolving as $\delta \sim a$.

(iv) Points $\mathcal{F}_\pm$ and $\mathcal{G}_\pm$ correspond to stiff DE-dominated solutions. Points $\mathcal{F}_\pm$ are always saddle, but points $\mathcal{G}_\pm$ can be either a saddle or stable node depending on $\lambda$ and the sign of $\gamma$. At the perturbation level, while points $\mathcal{F}_\pm$ correspond to a constant growth rate of matter perturbations, points $\mathcal{G}_\pm$ correspond to unstable growth. Finally, note that, while in the pure background analysis points $\mathcal{F}_\pm$ can be stable, the inclusion of perturbations makes them saddle.

(v) Points $\mathcal{H}$ and $\mathcal{I}$ correspond to DE-dominated solutions, which for $\lambda^2 < 2$ exhibit acceleration. Point $\mathcal{H}$ is stable at both the background and perturbation level when $\gamma > 0$ and $\lambda^2 < 4$, and similarly, point $\mathcal{I}$ is stable when $\gamma > 0$ and $\lambda^2 > 4$. Point $\mathcal{H}$ has a constant growth rate of matter perturbations, while point $\mathcal{I}$ corresponds to decay of matter perturbations in its stability region, while it corresponds to unstable perturbation growth when it is a saddle.

Similarly to the previous interacting model, we see that the inclusion of perturbations allows us to differentiate among critical points that are equivalent at the background level. Additionally, performing an analysis at infinity, we find that there are no extra critical points. From the combined analysis of the background and perturbation level, we find that point $\mathcal{E}_-$ is physically interesting for the description of the epoch where matter perturbations are generated, and the fact that it is saddle gives the natural exit from this phase. At late times, the physically interesting point is $\mathcal{H}$, which corresponds to DE-dominated accelerated solution with constant matter perturbations, in agreement with observations. For completeness, in Fig. 5, we depict the evolution of the growth rate $U$, which shows that for a wide range of initial conditions $\delta$ increases at intermediate redshifts and then asymptotically approaches a constant value (since $U$ goes to zero). Moreover, the precise evolution of matter growth depends on the interaction parameter $\gamma$ as expected.

## IV. CONCLUSIONS

Cosmological scenarios with interactions between DM and DE sectors are widely studied since they offer alleviation of the cosmic coincidence problem, and additionally, they may lead to solutions to the Hubble and $\sigma_8$ tensions. Hence, in the present work, we applied the formalism of dynamical system analysis to investigate the evolution of interacting scenarios both at the background and perturbation levels in a unified way.

We transformed the background and perturbation equations into an autonomous system and investigated them for two interaction forms. Since the resulting dynamical system contains the extra perturbation variable related to the matter overdensity, the critical points of the background analysis split into more points, corresponding to different behavior of matter perturbations, and hence to stability properties.

For both models, we obtained critical points describing a wide range of interesting cosmological solutions, corresponding to DM, scaling, or DE-dominated ones, accelerating and nonaccelerating, with decaying, constant, or growing matter perturbations. In particular, from the combined analysis of the background and perturbation equations, we found points that describe the nonaccelerating matter-dominated epoch with the correct growth of matter structure. The fact that they are saddle provides the natural exit from this phase. Furthermore, at late times, we found stable attractors that correspond to a DE-dominated accelerated solution with constant matter perturbations, as observations require it.

In summary, interacting cosmology, and more efficiently interacting model I, can correctly describe the matter and DE epochs at the background and perturbation levels. Moreover, we have an extra parameter to adjust both the background and perturbation behavior, namely, the coupling parameter. Hence, for suitable parameter regions, one can obtain the correct thermal history of the Universe, at both background and perturbation levels, offering a matter-dominated phase where matter perturbations grow, which ends naturally, and then the transition to the DE-dominated accelerating phase. These features reveal the significant effect of the interaction.

It would be interesting to investigate the phase space of both the background and perturbation levels in interacting scenarios in which dark energy has an effective origin, namely, instead of quintessence field to arise from modified gravity. Additionally, one could also apply the dynamical system analysis in the case of tensor perturbations. These studies lie beyond the scope of the present work and are left for future projects.

## ACKNOWLEDGMENTS

J. D. was supported by the Core Research Grant of SERB, Department of Science and Technology India (File No. CRG/2018/001035) and the Associate program of Inter-University Centre for Astronomy and Astrophysics. S. B. and E. N. S. would like to acknowledge the contribution of the COST Action CA18108 "Quantum Gravity Phenomenology in the multi-messenger approach."

[1] E. N. Saridakis *et al.* (CANTATA Collaboration), Modified gravity and cosmology: An update by the CANTATA network, arXiv:2105.12582.
[2] S. Capozziello and M. De Laurentis, Extended theories of gravity, Phys. Rep. **509**, 167 (2011).
[3] Y.-F. Cai, S. Capozziello, M. De Laurentis, and E. N. Saridakis, f(T) teleparallel gravity and cosmology, Rep. Prog. Phys. **79**, 106901 (2016).
[4] E. J. Copeland, M. Sami, and S. Tsujikawa, Dynamics of dark energy, Int. J. Mod. Phys. D **15**, 1753 (2006).
[5] Y.-F. Cai, E. N. Saridakis, M. R. Setare, and J.-Q. Xia, Quintom Cosmology: Theoretical implications and observations, Phys. Rep. **493**, 1 (2010).
[6] T. Damour and A. M. Polyakov, The string dilaton and a least coupling principle, Nucl. Phys. **B423**, 532 (1994).
[7] L. P. Chimento, A. S. Jakubi, D. Pavon, and W. Zimdahl, Interacting quintessence solution to the coincidence problem, Phys. Rev. D **67**, 083513 (2003).
[8] A. Pourtsidou and T. Tram, Reconciling CMB and structure growth measurements with dark energy interactions, Phys. Rev. D **94**, 043518 (2016).
[9] R. An, C. Feng, and B. Wang, Relieving the tension between weak lensing and cosmic microwave background with interacting dark matter and dark energy models, J. Cosmol. Astropart. Phys. 02 (2018) 038.
[10] S. Kumar and R. C. Nunes, Echo of interactions in the dark sector, Phys. Rev. D **96**, 103511 (2017).
[11] W. Yang, A. Mukherjee, E. Di Valentino, and S. Pan, Interacting dark energy with time varying equation of state and the $H_0$ tension, Phys. Rev. D **98**, 123527 (2018).
[12] E. Di Valentino *et al.*, Cosmology intertwined III: $f\sigma_8$ and $S_8$, Astropart. Phys. **131**, 102604 (2021).
[13] E. Di Valentino *et al.*, Snowmass2021—Letter of interest cosmology intertwined II: The hubble constant tension, Astropart. Phys. **131**, 102605 (2021).
[14] E. Di Valentino, O. Mena, S. Pan, L. Visinelli, W. Yang, A. Melchiorri, D. F. Mota, A. G. Riess, and J. Silk, In the realm of the Hubble tension—a review of solutions, Classical Quantum Gravity **38**, 153001 (2021).
[15] J. D. Barrow and T. Clifton, Cosmologies with energy exchange, Phys. Rev. D **73**, 103520 (2006).
[16] L. Amendola, G. Camargo Campos, and R. Rosenfeld, Consequences of dark matter-dark energy interaction on cosmological parameters derived from SNIa data, Phys. Rev. D **75**, 083506 (2007).
[17] J.-H. He and B. Wang, Effects of the interaction between dark energy and dark matter on cosmological parameters, J. Cosmol. Astropart. Phys. 06 (2008) 010.
[18] S. Basilakos and M. Plionis, Is the interacting dark matter scenario an alternative to dark energy?, Astron. Astrophys. **507**, 47 (2009).
[19] M. B. Gavela, D. Hernandez, L. Lopez Honorez, O. Mena, and S. Rigolin, Dark coupling, J. Cosmol. Astropart. Phys. 07 (2009) 034; 05 (2010) E01.
[20] X.-M. Chen, Y. Gong, E. N. Saridakis, and Y. Gong, Time-dependent interacting dark energy and transient acceleration, Int. J. Theor. Phys. **53**, 469 (2014).
[21] A. Pourtsidou, C. Skordis, and E. J. Copeland, Models of dark matter coupled to dark energy, Phys. Rev. D **88**, 083505 (2013).
[22] W. Yang and L. Xu, Coupled dark energy with perturbed Hubble expansion rate, Phys. Rev. D **90**, 083532 (2014).
[23] R. C. Nunes and E. M. Barboza, Dark matter-dark energy interaction for a time-dependent EoS parameter, Gen. Relativ. Gravit. **46**, 1820 (2014).
[24] V. Faraoni, J. B. Dent, and E. N. Saridakis, Covariantizing the interaction between dark energy and dark matter, Phys. Rev. D **90**, 063510 (2014).
[25] V. Salvatelli, N. Said, M. Bruni, A. Melchiorri, and D. Wands, Indications of a Late-Time Interaction in the Dark Sector, Phys. Rev. Lett. **113**, 181301 (2014).
[26] S. Pan, S. Bhattacharya, and S. Chakraborty, An analytic model for interacting dark energy and its observational constraints, Mon. Not. R. Astron. Soc. **452**, 3038 (2015).

[27] C. G. Boehmer, N. Tamanini, and M. Wright, Interacting quintessence from a variational approach Part I: algebraic couplings, Phys. Rev. D **91**, 123002 (2015).
[28] R. C. Nunes, S. Pan, and E. N. Saridakis, New constraints on interacting dark energy from cosmic chronometers, Phys. Rev. D **94**, 023508 (2016).
[29] C. G. Boehmer, N. Tamanini, and M. Wright, Interacting quintessence from a variational approach Part II: derivative couplings, Phys. Rev. D **91**, 123003 (2015).
[30] A. Mukherjee and N. Banerjee, In search of the dark matter dark energy interaction: A kinematic approach, Classical Quantum Gravity **34**, 035016 (2017).
[31] R.-G. Cai, N. Tamanini, and T. Yang, Reconstructing the dark sector interaction with LISA, J. Cosmol. Astropart. Phys. 05 (2017) 031.
[32] W. Yang, S. Pan, and J. D. Barrow, Large-scale stability and astronomical constraints for coupled dark-energy models, Phys. Rev. D **97**, 043529 (2018).
[33] L. Santos, W. Zhao, E. G. M. Ferreira, and J. Quintin, Constraining interacting dark energy with CMB and BAO future surveys, Phys. Rev. D **96**, 103529 (2017).
[34] S. Pan, A. Mukherjee, and N. Banerjee, Astronomical bounds on a cosmological model allowing a general interaction in the dark sector, Mon. Not. R. Astron. Soc. **477**, 1189 (2018).
[35] D. Grandon and V. H. Cardenas, Exploring evidence of interaction between dark energy and dark matter, arXiv: 1804.03296.
[36] R. von Marttens, L. Casarini, D. F. Mota, and W. Zimdahl, Cosmological constraints on parametrized interacting dark energy, Phys. Dark Universe **23**, 100248 (2019).
[37] M. Bonici and N. Maggiore, Constraints on interacting dynamical dark energy and a new test for ΛCDM, Eur. Phys. J. C **79**, 672 (2019).
[38] C. Li, X. Ren, M. Khurshudyan, and Y.-F. Cai, Implications of the possible 21-cm line excess at cosmic dawn on dynamics of interacting dark energy, Phys. Lett. B **801**, 135141 (2020).
[39] W. Yang, S. Pan, E. Di Valentino, B. Wang, and A. Wang, Forecasting interacting vacuum-energy models using gravitational waves, J. Cosmol. Astropart. Phys. 05 (2020) 050.
[40] A. Al Mamon, A. Paliathanasis, and S. Saha, Dynamics of an interacting barrow holographic dark energy model and its thermodynamic implications, Eur. Phys. J. Plus **136**, 134 (2021).
[41] J. B. Jiménez, D. Bettoni, D. Figueruelo, F. A. T. Pannia, and S. Tsujikawa, Velocity-dependent interacting dark energy and dark matter with a Lagrangian description of perfect fluids, J. Cosmol. Astropart. Phys. 03 (2021) 085.
[42] M. Lucca, Multi-interacting dark energy and its cosmological implications, Phys. Rev. D **104**, 083510 (2021).
[43] S. Konitopoulos, E. N. Saridakis, P. C. Stavrinos, and A. Triantafyllopoulos, Dark gravitational sectors on a generalized scalar-tensor vector bundle model and cosmological applications, Phys. Rev. D **104**, 064018 (2021).
[44] Yu. L. Bolotin, A. Kostenko, O. A. Lemets, and D. A. Yerokhin, Cosmological evolution with interaction between dark energy and dark matter, Int. J. Mod. Phys. D **24**, 1530007 (2015).
[45] B. Wang, E. Abdalla, F. Atrio-Barandela, and D. Pavon, Dark matter and dark energy interactions: Theoretical challenges, cosmological implications and observational signatures, Rep. Prog. Phys. **79**, 096901 (2016).
[46] E. Abdalla, L. R. Abramo, L. Sodre, Jr., and B. Wang, Signature of the interaction between dark energy and dark matter in galaxy clusters, Phys. Lett. B **673**, 107 (2009).
[47] J.-H. He, B. Wang, and E. Abdalla, Testing the interaction between dark energy and dark matter via latest observations, Phys. Rev. D **83**, 063515 (2011).
[48] F. C. Solano and U. Nucamendi, Reconstruction of the interaction term between dark matter and dark energy using SNe Ia, J. Cosmol. Astropart. Phys. 04 (2012) 011.
[49] S. Cao and N. Liang, Interaction between dark energy and dark matter: Observational constraints from ohd, bao, cmb and sne ia, Int. J. Mod. Phys. D **22**, 1350082 (2013).
[50] A. A. Costa, X.-D. Xu, B. Wang, E. G. M. Ferreira, and E. Abdalla, Testing the interaction between dark energy and dark matter with planck data, Phys. Rev. D **89**, 103531 (2014).
[51] S. Pan, W. Yang, C. Singha, and E. N. Saridakis, Observational constraints on sign-changeable interaction models and alleviation of the $H_0$ tension, Phys. Rev. D **100**, 083539 (2019).
[52] S. Pan, W. Yang, E. Di Valentino, E. N. Saridakis, and S. Chakraborty, Interacting scenarios with dynamical dark energy: Observational constraints and alleviation of the $H_0$ tension, Phys. Rev. D **100**, 103520 (2019).
[53] G. Cheng, Y.-Z. Ma, F. Wu, J. Zhang, and X. Chen, Testing interacting dark matter and dark energy model with cosmological data, Phys. Rev. D **102**, 043517 (2020).
[54] S. Pan, G. S. Sharov, and W. Yang, Field theoretic interpretations of interacting dark energy scenarios and recent observations, Phys. Rev. D **101**, 103533 (2020).
[55] W. Yang, S. Pan, L. A. Saló, and J. de Haro, Theoretical and observational bounds on some interacting vacuum energy scenarios, Phys. Rev. D **103**, 083520 (2021).
[56] J. Dutta, W. Khyllep, and N. Tamanini, Dark energy with a gradient coupling to the dark matter fluid: cosmological dynamics and structure formation, J. Cosmol. Astropart. Phys. 01 (2018) 038.
[57] W. Khyllep and J. Dutta, Linear growth index of matter perturbations in Rastall gravity, Phys. Lett. B **797**, 134796 (2019).
[58] W. Khyllep, A. Paliathanasis, and J. Dutta, Cosmological solutions and growth index of matter perturbations in $f(Q)$ gravity, Phys. Rev. D **103**, 103521 (2021).
[59] A. Paliathanasis, G. Leon, W. Khyllep, J. Dutta, and S. Pan, Interacting quintessence in light of generalized uncertainty principle: cosmological perturbations and dynamics, Eur. Phys. J. C **81**, 607 (2021).
[60] G. Caldera-Cabral, R. Maartens, and B. M. Schaefer, The growth of structure in interacting dark energy models, J. Cosmol. Astropart. Phys. 07 (2009) 027.
[61] S. Tsujikawa, A. De Felice, and J. Alcaniz, Testing for dynamical dark energy models with redshift-space distortions, J. Cosmol. Astropart. Phys. 01 (2013) 030.
[62] Y.-H. Li, J.-F. Zhang, and X. Zhang, Exploring the full parameter space for an interacting dark energy model with recent observations including redshift-space distortions:

Application of the parametrized post-friedmann approach, Phys. Rev. D **90**, 123007 (2014).
[63] J. Wainwright and G. F. R. Ellis, *Dynamical Systems in Cosmology* (Cambridge University Press, Cambridge, England, 1997).
[64] A. A. Coley, *Dynamical systems and cosmology* (Kluwer, Dordrecht, Netherlands, 2003).
[65] S. Bahamonde, C. G. Böhmer, S. Carloni, E. J. Copeland, W. Fang, and N. Tamanini, Dynamical systems applied to cosmology: Dark energy and modified gravity, Phys. Rep. **775–777**, 1 (2018).
[66] E. J. Copeland, A. R. Liddle, and D. Wands, Exponential potentials and cosmological scaling solutions, Phys. Rev. D **57**, 4686 (1998).
[67] Y. Gong, A. Wang, and Y.-Z. Zhang, Exact scaling solutions and fixed points for general scalar field, Phys. Lett. B **636**, 286 (2006).
[68] M. R. Setare and E. N. Saridakis, Quintom dark energy models with nearly flat potentials, Phys. Rev. D **79**, 043005 (2009).
[69] T. Matos, J.-R. Luevano, I. Quiros, L. A. Urena-Lopez, and J. A. Vazquez, Dynamics of Scalar Field Dark Matter With a Cosh-like Potential, Phys. Rev. D **80**, 123521 (2009).
[70] E. J. Copeland, S. Mizuno, and M. Shaeri, Dynamics of a scalar field in Robertson-Walker spacetimes, Phys. Rev. D **79**, 103515 (2009).
[71] Y. Leyva, D. Gonzalez, T. Gonzalez, T. Matos, and I. Quiros, Dynamics of a self-interacting scalar field trapped in the braneworld for a wide variety of self-interaction potentials, Phys. Rev. D **80**, 044026 (2009).
[72] G. Leon and E. N. Saridakis, Dynamics of the anisotropic Kantowsky-Sachs geometries in $R^n$ gravity, Classical Quantum Gravity **28**, 065008 (2011).
[73] L. A. Urena-Lopez, Unified description of the dynamics of quintessential scalar fields, J. Cosmol. Astropart. Phys. 03 (2012) 035.
[74] G. Leon, J. Saavedra, and E. N. Saridakis, Cosmological behavior in extended nonlinear massive gravity, Classical Quantum Gravity **30**, 135001 (2013).
[75] C. R. Fadragas, G. Leon, and E. N. Saridakis, Dynamical analysis of anisotropic scalar-field cosmologies for a wide range of potentials, Classical Quantum Gravity **31**, 075018 (2014).
[76] W. Khyllep and J. Dutta, Cosmological dynamics and bifurcation analysis of the general non-minimal coupled scalar field models, Eur. Phys. J. C **81**, 774 (2021).
[77] H. Zonunmawia, W. Khyllep, J. Dutta, and L. Järv, Cosmological dynamics of brane gravity: A global dynamical system perspective, Phys. Rev. D **98**, 083532 (2018).
[78] J. Dutta, W. Khyllep, and N. Tamanini, Scalar-Fluid interacting dark energy: Cosmological dynamics beyond the exponential potential, Phys. Rev. D **95**, 023515 (2017).
[79] J. Dutta, W. Khyllep, and N. Tamanini, Cosmological dynamics of scalar fields with kinetic corrections: Beyond the exponential potential, Phys. Rev. D **93**, 063004 (2016).
[80] A. P. Billyard and A. A. Coley, Interactions in scalar field cosmology, Phys. Rev. D **61**, 083503 (2000).
[81] X.-M. Chen, Y.-G. Gong, and E. N. Saridakis, Phase-space analysis of interacting phantom cosmology, J. Cosmol. Astropart. Phys. 04 (2009) 001.
[82] C. G. Boehmer, G. Caldera-Cabral, R. Lazkoz, and R. Maartens, Dynamics of dark energy with a coupling to dark matter, Phys. Rev. D **78**, 023505 (2008).
[83] A. Woszczyna, A dynamical systems approach to cosmological structure formation—Newtonian universe, Mon. Not. R. Astron. Soc. **255**, 701 (1992).
[84] A. Woszczyna, Gauge invariant cosmic structures: A Dynamic systems approach, Phys. Rev. D **45**, 1982 (1992).
[85] M. Bruni, Stability of open Universes, Phys. Rev. D **47**, 738 (1993).
[86] M. Bruni and K. Piotrkowska, Dust—radiation universes: Stability analysis, Mon. Not. R. Astron. Soc. **270**, 630 (1994).
[87] P. K. S. Dunsby, Covariant perturbations of anisotropic cosmological models, Phys. Rev. D **48**, 3562 (1993).
[88] S. Hobbs and P. K. S. Dunsby, Dynamical systems approach to magnetized cosmological perturbations, Phys. Rev. D **62**, 124007 (2000).
[89] A. Alho and F. C. Mena, Covariant and gauge-invariant linear scalar perturbations in multiple scalar field cosmologies, Phys. Rev. D **90**, 043501 (2014).
[90] S. Basilakos, G. Leon, G. Papagiannopoulos, and E. N. Saridakis, Dynamical system analysis at background and perturbation levels: Quintessence in severe disadvantage comparing to ΛCDM, Phys. Rev. D **100**, 043524 (2019).
[91] A. Alho, C. Uggla, and J. Wainwright, Perturbations of the Lambda-CDM model in a dynamical systems perspective, J. Cosmol. Astropart. Phys. 09 (2019) 045.
[92] R. G. Landim, Cosmological perturbations and dynamical analysis for interacting quintessence, Eur. Phys. J. C **79**, 889 (2019).
[93] C.-P. Ma and E. Bertschinger, Cosmological perturbation theory in the synchronous and conformal Newtonian gauges, Astrophys. J. **455**, 7 (1995).
[94] J. Valiviita, E. Majerotto, and R. Maartens, Instability in interacting dark energy and dark matter fluids, J. Cosmol. Astropart. Phys. 07 (2008) 020.
[95] E. N. Saridakis, Do we need soft cosmology?, Phys. Lett. B **822**, 136649 (2021).
[96] E. N. Saridakis, W. Yang, S. Pan, F. K. Anagnostopoulos, and S. Basilakos, Observational constraints on soft dark energy and soft dark matter: challenging ΛCDM, arXiv: 2112.08330.
[97] J.-H. He, B. Wang, and E. Abdalla, Stability of the curvature perturbation in dark sectors' mutual interacting models, Phys. Lett. B **671**, 139 (2009).
[98] B. M. Jackson, A. Taylor, and A. Berera, On the large-scale instability in interacting dark energy and dark matter fluids, Phys. Rev. D **79**, 043526 (2009).
[99] M. B. Gavela, L. Lopez Honorez, O. Mena, and S. Rigolin, Dark Coupling and Gauge Invariance, J. Cosmol. Astropart. Phys. 11 (2010) 044.

[100] R. Cen, Decaying cold dark matter model and small-scale power, Astrophys. J. Lett. **546**, L77 (2001).
[101] M. Oguri, K. Takahashi, H. Ohno, and K. Kotake, Decaying cold dark matter and the evolution of the cluster abundance, Astrophys. J. **597**, 645 (2003).
[102] K. A. Malik, D. Wands, and C. Ungarelli, Large scale curvature and entropy perturbations for multiple interacting fluids, Phys. Rev. D **67**, 063516 (2003).
[103] H. Ziaeepour, Quintessence from the decay of a superheavy dark matter, Phys. Rev. D **69**, 063512 (2004).